horticulturae

MDPI

Article

Genome–Wide Investigation of the CBL–CIPK Gene Family in Oil Persimmon: Evolution, Function and Expression Analysis during Development and Stress

Cuiyu Liu [1,2], Yanpeng Wang [1,2], Jin Yao [3], Xu Yang [1,2], Kaiyun Wu [1,2], Guoxin Teng [3], Bangchu Gong [1,2,*] and Yang Xu [1,2,*]

[1] Research Institute of Subtropical Forestry, Chinese Academy of Forestry, Hangzhou 311400, China
[2] Zhejiang Provincial Key Laboratory of Tree Breeding, Hangzhou 311400, China
[3] Lanxi City Nursery of Zhejiang Provence, Lanxi 321100, China
* Correspondence: gongbc@126.com (B.G.); xuyang198610@163.com (Y.X.)

Abstract: Ca^{2+}-sensors, calcineurin B-like proteins (CBLs), and calcineurin B-like protein-interacting protein kinases (CIPKs) form a CBL–CIPK complex to regulate signal transduction. This study aimed to reveal the characteristics of the CBL–CIPK gene family in oil persimmon (*Diospyros oleifera*). Ten *DoCBL* and 23 *DoCIPK* genes were identified, and gene duplication among them was mainly attributed to segmental duplication. According to phylogenetic and structural analysis, DoCBLs were clustered into four groups with distinct motifs, namely myristoylation and palmytoylation sites in their N-terminus, and *DoCIPKs* containing a NAF/FISL domain were clustered into intron-rich and intron-less groups. The expression patterns of *DoCBLs* and *DoCIPKs* were tissue- and time-specific in different tissues and at different stages of fruit development. Most *CBL–CIPK* genes were upregulated under NaCl, drought, and $Ca(NO_3)_2$ stress using qRT-PCR analysis. DoCBL5 and DoCIPK05 were both located in the plasma membrane of cells using green fusion proteins (GFP) in tobacco leaves. DoCBL5 and DoCIPK05 might interact with AKT1, PP2C, and SNF to regulate the Ca^{2+} signals, K^+, and ABA homeostasis in cells. In conclusion, these results suggested that the CBL–CIPK family genes might play important roles in oil persimmon growth and stress responses.

Keywords: oil persimmon; CBL–CIPK genes; evolution analysis; expression pattern; subcellular location

Citation: Liu, C.; Wang, Y.; Yao, J.; Yang, X.; Wu, K.; Teng, G.; Gong, B.; Xu, Y. Genome–Wide Investigation of the CBL–CIPK Gene Family in Oil Persimmon: Evolution, Function and Expression Analysis during Development and Stress. *Horticulturae* **2023**, *9*, 30. https://doi.org/10.3390/horticulturae9010030

Academic Editors: Junbei Ni, Aidi Zhang, Minjie Qian and Nakao Kubo

Received: 24 October 2022
Revised: 7 December 2022
Accepted: 16 December 2022
Published: 27 December 2022

1. Introduction

Ca^{2+}, one of the main cell wall components, serves as a universal second messenger and plays crucial roles in plant growth and development [1,2], as well as the plant responses to abiotic/biotic stresses [3]. The changes in cytosolic Ca^{2+} concentration ($[Ca^{2+}]_{cyt}$) evoke many changes in cellular processes, such as cell division, cell elongation, cell differentiation, photomorphogenesis, defense, and stress responses in plant cells [4]. Ca^{2+}-sensors, calcineurin B-like proteins (CBLs), and calcineurin B-like protein-interacting protein kinases (CIPKs) interact with each other and form CBL–CIPK complexes. These complexes are involved in multiple signal transduction pathways during mechanical stimulation, pathogen attack, reactive oxygen species (ROS) burst, salinity, drought, heat, and cold stress.

As a structural basis for Ca^{2+} binding, CBL proteins harbor four conserved elongation factor-hands (EF-hands), which consist of two α helices connected by a loop of 12 amino acids [5]. EF-hands are Ca^{2+}-sensors characterized by the presence of a conserved Asp (D) or Glu (E) residue [6]. Many CBL proteins also contain conserved MGCXXS/T motifs with a conserved myristoylation site and palmytoylation site in their N-terminal regions. These CBLs are anchored in cell membranes to transduce Ca^{2+} signals [7,8]. The CIPK gene family contains a conserved regulatory domain in the C-terminus and a conserved Ser–Thr kinase domain in the N-terminus. Within the regulatory C-terminal domain, a 24 amino acid domain NAF/FISL is unique to CIPKs and is required and sufficient for interaction

with CBLs [9]. The NAF domain has been named after the prominent conserved amino acids Asn–Ala–Phe [9]. In addition, the protein–phosphatase interaction (PPI) domain within the C-terminus of CIPKs also targets specific members of the protein phosphatase 2C (PP2C) family [10]. However, the Ser–Thr kinases are similar in structure to the SNF1 protein kinases and AMO–dependent protein kinases [9]. Thus, the Ser–Thr kinase, NAF domain and PPI domain are basic characters of CIPK gene family.

CBL–CIPK complexes have been reported to coordinate stress responses and participate in transport of Na^+, K^+ and H^+ in plant cells [2]. Among 10 CBLs and 26 CIPKs in *Arabidopsis thaliana*, the initial functional analysis of CBL–CIPK networks was conducted on the salt overly sensitive (SOS) pathway [11]. In the SOS pathway, AtCBL4/SOS3 and AtCIPK24/SOS2 modulate the activity of SOS1 (a plasma membrane Na^+/H^+ antiporter) and NHX1 (a vacuolar Na^+/H^+ antiporter) to remove excess Na^+ either by extrusion from the cytoplasm or by sequestration into the vacuole [12,13]. AtCBL10 plays a critical role in the activation of Na^+ compartmentation into the vacuole. Yang et al. [14] found that *cbl10* and *cipk24* double mutants were more sensitive than the *cipk24* single mutant, suggesting that CBL10 directs a process involving CIPK24 and other partners different from the SOS pathway. AtCBL1 and AtCBL9 interact with AtCIPK23, and these complexes regulate the activity of the K^+ transporter AKT1 [15]. Moreover, AtCIPK6 and AtCIPK16 both activate AKT1 in a CBL–dependent manner [16]. In rice (Os) and grapevine (Vv), the OsCBL1–OsCIK23 and VvCBL01–VvCIPK04 modules (orthologs of AtCBL1 and AtCIPK23) were also reported to enhance AKT1–mediated K^+ uptake [17,18]. Functional homology between the CBL–CIPK modules in different species indicates that the canonical CBL–CIPK signal transduction pathway might be conserved across species [5]. It is worth noting that the subcellular location of the CBL–CIPK module is determined by its interacting CBL partner. AtCBL1 and AtCBL9 target AtCIPK23 to the plasma membrane (PM), and other individual AtCBLs can target AtCIPK23 to different cellular locations, thereby directing the same kinase to have distinct functions [19]. In rice (*Oryza sativa*), many *OsCIPK* genes have diverse roles in different stress responses, and overexpression of *OsCIPK03*, *OsCIPK12*, and *OsCIPK15* significantly improves plant tolerance to cold, drought, and salt stress, respectively [20]. *TaCBL* and *TaCIPK* genes of wheat (*Triticum aestivum*) were differentially expressed in different tissues and under different abiotic stresses [21]. Most *MdCIPK* genes of apple (*Malus domestica*) play different roles in leaf, root, flower and fruit development [22]. Most *PbCIPKs* of pear (*Pyrus bretschneideri*) play important roles in the abiotic stress responses, e.g., PbCIPK22, -19, -18, -15, -8, and -6 can serve as core regulators in response to salt and osmotic stresses based on co-expression networks of PbCIPKs [23]. These results suggested structural and functional distinctions among CBL–CIPK family genes.

Diospyros, from the Ebenaceae family, is a plant genus that includes over 500 species widely distributed across tropical and subtropical regions [24]. Among these species, oil persimmon (*Diospyros oleifera*) has a strong resistance to abiotic stresses, plant diseases, and insect pests [25], and it can be used as a model plant for the genus Diospyros based on stress responses and morphological, physiological, and molecular biological studies [26]. Due to the great significance of CBL–CIPK networks in various biological processes and stress responses, it is indispensable to explore the characteristics of *CBL–CIPK* genes, which have been reported rarely in persimmon or Diospyros. In this study, sequence and evolution analyses of *CBL–CIPK* genes were conducted using the available oil persimmon genome [27]. The expression profiles of *CBL–CIPK* genes were also determined in different oil persimmon tissues and at various stages of fruit development, as well as in the response to abiotic stresses. In addition, the subcellular locations of DoCBL5 and DoCIPK05 were detected using a GFP fusion protein in tobacco leaves. Through this work, we will better understand the roles of *CBL–CIPK* genes in oil persimmon growth and stress responses. This study will also provide new insights into the functions of the CBL–CIPK gene family in Diospyros and offer a reference for persimmon genetic breeding purposes.

2. Results

2.1. Identification of CBL–CIPK Genes in Oil Persimmon

An EF-hand domain (PS50222) and NAF domain (PF03822) were employed to identify the putative DoCBL and DoCIPK proteins from the oil persimmon genome, respectively. The results showed that ten putative DoCBLs contained three conserved EF–hands, and all 23 putative DoCIPKs contained a highly conserved NAF domain, PPI domain (except DoCIPK09) and Ser–Thr kinases (Table 1). The length of DoCBLs ranged from 213 aa to 252 aa, except DoCBL7 (383 aa), and that of DoCIPKs ranged from 396 aa to 494 aa, except DoCIPK09 (350 aa) (Table 1). The predicted Mw values of the DoCBL and DoCIPK proteins ranged from 24.40 to 44.49 kDa and 39.43 to 55.22 kDa, respectively. Overall, the pI of all DoCBL proteins was less than seven except DoCBL7, while 82.6% of the DoCIPK proteins had a pI greater than seven. Therefore, DoCBLs were rich in acidic amino acids and DoCIPKs were rich in basic amino acids. Additionally, seven DoCBLs had myristoylation sites (Gly) at the second or the seventh position in their N-terminus. Three DoCBLs (DoCBL1, DoCBL2 and DoCBL10) had palmitoylation sites (Cys) at the fourth position in their N-terminus, while DoCBL5, DoCBL8 and DoCBL9 had N-terminal Cys at the third, eighteenth and/or twelfth positions (Table 1). The Cys amino acid at the third position in the N-terminus was included in the conserved MGCXXS/T motif. Meanwhile, 22 DoCIPKs had three conserved domains, Ser–Thr kinases, NAF domains, and PPI domains, while DoCIPK09 lost its PPI domain within the C-terminus due to the incorrect assembly of the oil persimmon genome. The results showed that the protein length, protein property, and structures of DoCBLs and DoCIPKs were highly conserved.

Table 1. Characteristics of CBL–CIPK genes identified from oil persimmon.

Gene ID	Name	Length	Mw * (kDa)	pI *	Arabidopsis Orthologs	EF—Hands	Cys Amino Acid Location	Gly Amino Acid Location
EVM0026572.3	DoCBL1	225	25.8	5.46	AT4G26570.1	3	C (4, 18)	G (7)
EVM0017523.1	DoCBL2	226	26.05	4.93	AT4G26570.1	3	C (4, 12, 18)	G (7)
EVM0005359.2	DoCBL3	252	29.13	5.02	AT5G24270.1	3	/	G (2)
EVM0012501.1	DoCBL4	249	28.72	4.82	AT4G26570.1	3	C (7, 9)	/
EVM0016230.1	DoCBL5	213	24.4	4.74	AT4G17615.2	3	C (3)	G (2)
EVM0025671.1	DoCBL6	218	24.75	5.04	AT1G64480.1	3	C (20, 40)	G (7)
EVM0028457.1	DoCBL7	383	44.49	9.1	AT4G26570.1	3	C (32, 46)	/
EVM0015273.1	DoCBL8	213	24.4	4.74	AT4G17615.1	3	C (3)	G (2)
EVM0011958.1	DoCBL9	213	24.4	4.74	AT4G17615.2	3	C (3)	G (2)
EVM0006583.2	DoCBL10	226	26.34	4.89	AT4G26570.1	3	C (4, 12, 18)	/
Gene ID	**Name**	**Length**	**Mw * (kDa)**	**pI ***	**Arabidopsis Orthologs**		**Domains**	
EVM0026935.1	DoCIPK01	446	50.31	7.98	AT5G10930.1		Ser–Thr kinases, NAF, PPI	
EVM0017998.1	DoCIPK02	429	48.22	8.48	AT2G30360.1		Ser–Thr kinases, NAF, PPI	
EVM0029929.1	DoCIPK03	472	53.17	8.57	AT5G58380.1		Ser–Thr kinases, NAF, PPI	
EVM0019494.1	DoCIPK04	478	53.27	8.35	AT1G30270.1		Ser–Thr kinases, NAF, PPI	
EVM0027553.1	DoCIPK05	425	47.57	9.2	AT4G30960.1		Ser–Thr kinases, NAF, PPI	
EVM0031579.3	DoCIPK06	494	55.22	7.64	AT4G18700.1		Ser–Thr kinases, NAF, PPI	
EVM0007664.1	DoCIPK07	430	47.93	9.31	AT5G45820.1		Ser–Thr kinases, NAF, PPI	
EVM0005656.1	DoCIPK08	471	53.09	8.84	AT4G18700.1		Ser–Thr kinases, NAF, PPI	
EVM0030600.1	DoCIPK09	350	39.43	8.96	AT1G30270.1		Ser–Thr kinases, NAF	
EVM0006423.1	DoCIPK10	469	53.51	9.15	AT5G58380.1		Ser–Thr kinases, NAF, PPI	
EVM0006143.1	DoCIPK11	445	50.09	8.63	AT5G01810.1		Ser–Thr kinases, NAF, PPI	
EVM0019559.1	DoCIPK12	441	49.61	8.23	AT5G35410.1		Ser–Thr kinases, NAF, PPI	
EVM0031872.1	DoCIPK13	446	49.72	8.98	AT4G30960.1		Ser–Thr kinases, NAF, PPI	
EVM0005984.1	DoCIPK14	453	51.28	5.77	AT5G57630.1		Ser–Thr kinases, NAF, PPI	
EVM0022207.1	DoCIPK15	422	46.34	9.45	AT3G23000.1		Ser–Thr kinases, NAF, PPI	
EVM0020525.1	DoCIPK16	446	50.79	6.88	AT4G24400.1		Ser–Thr kinases, NAF, PPI	
EVM0016074.1	DoCIPK17	455	51.25	8.82	AT5G58380.1		Ser–Thr kinases, NAF, PPI	

Table 1. *Cont.*

Gene ID	Name	Length	Mw * (kDa)	pI *	Arabidopsis Orthologs	Domains
EVM0026193.1	DoCIPK18	438	49.49	8.63	AT5G01820.1	Ser–Thr kinases, NAF, PPI
EVM0014392.1	DoCIPK19	429	47.64	8.43	AT3G23000.1	Ser–Thr kinases, NAF, PPI
EVM0019419.1	DoCIPK20	453	51.09	9.42	AT5G58380.1	Ser–Thr kinases, NAF, PPI
EVM0016829.1	DoCIPK21	422	47.83	8.38	AT2G30360.1	Ser–Thr kinases, NAF, PPI
EVM0009367.1	DoCIPK22	396	44.68	6.69	AT1G30270.1	Ser–Thr kinases, NAF, PPI
EVM0000183.1	DoCIPK23	432	48.63	6.35	AT3G17510.1	Ser–Thr kinases, NAF, PPI

* Molecular weight (Mw); isoelectric points (pI); /: not contained.

2.2. Phylogenetic Analysis of the CBL–CIPK Gene Family

To determine the evolutionary relationships and functional associations, maximum likelihood (ML) phylogenetic trees were constructed using the full-length protein sequences of CBL and CIPK from six plants, including *Diospyros oleifera*, *Arabidopsis thaliana*, *Actinidia chinensis*, *Malus domestica*, *Solanum lycopersicum* and *Vitis vinifera* (Figure 1). The phylogenetic tree showed that DoCBLs were clustered into four groups, which was consistent with the presence of conserved amino acids Gly and Cys on their N-termini. There were three DoCBLs (DoCBL1/2/10) in Group I, two DoCBLs in Group II (DoCBL4/7, bootstrap, BS = 90%), three DoCBLs (DoCBL5/8/9) in Group III (BS = 87%), and two DoCBLs (DoCBL3/6) in Group IV (Figure 1a). The phylogenetic tree of the CIPK gene family was divided into two groups with a great difference in intron numbers between them. Group I (Intron-less) contained 16 DoCIPK proteins, and Group II (Intron-rich) contained seven DoCIPKs (Figure 1b, BS = 93%). These results indicated that members of the CBL and CIPK gene families belonging to the same group might have similar structural and functional characteristics.

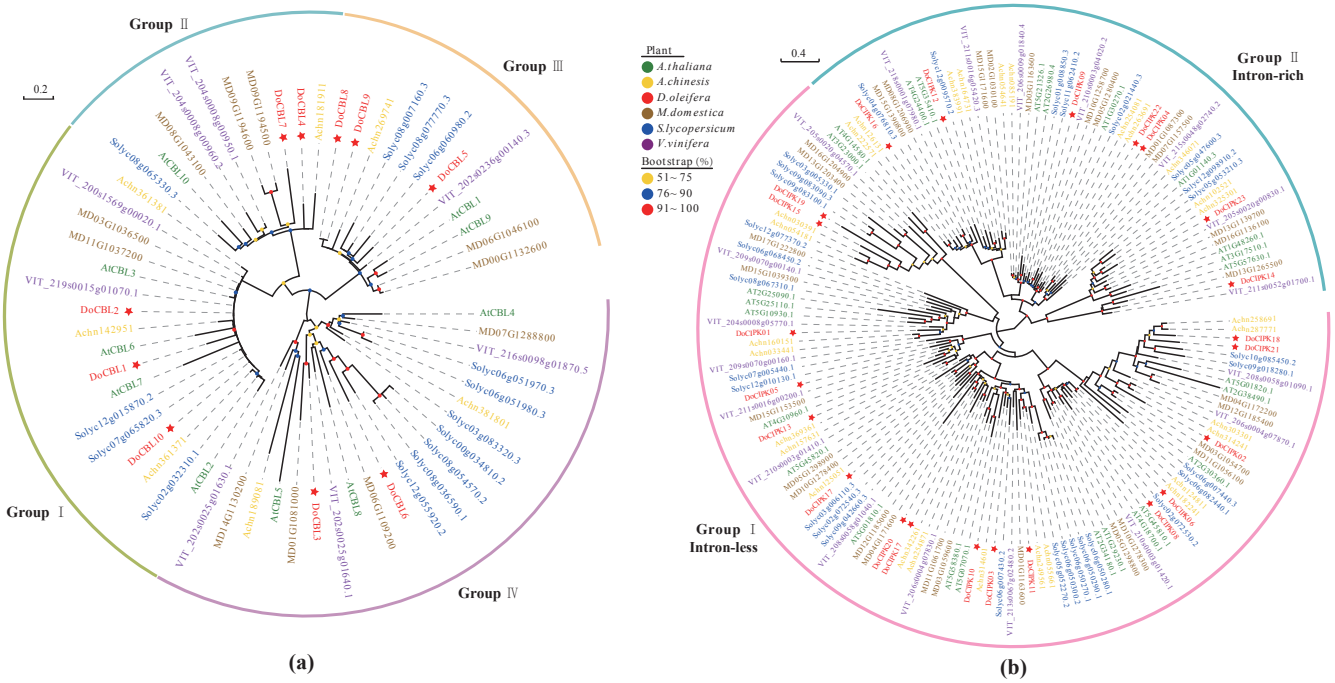

Figure 1. Phylogenetic trees of CBL proteins (**a**) and CIPK proteins (**b**) from *Diospyros oleifera*, *Arabidopsis thaliana*, *Actinidia chinensis*, *Malus domestica*, *Solanum lycopersicum* and *Vitis vinifera*. The different colored arcs indicate different groups. Proteins from the six plants are denoted by different colors. Node support values (pots) are quantified by approximate likelihood ratio test (aLRT) statistics with the SH–like procedure. DoCBLs and DoCIPKs are marked with red stars.

2.3. Chromosomal Location and Gene Duplication

The locations of *DoCBLs* and *DoCIPKs* were marked on the oil persimmon chromosomes to investigate their genomic distribution. As shown in Figure 2, the chromosomal location analysis revealed that ten *DoCBLs* were mapped onto six chromosomes, while 23 *DoCIPKs* were mapped onto ten chromosomes. However, the distribution of *DoCBL* and *DoCIPK* genes on the chromosomes was uneven. Chromosomes 2, 8, 10, and 15 each had one *DoCBL* gene, chromosome 13 had two *DoCBLs*, and chromosome 14 had four *DoCBLs* (Figure 2). Chromosomes 1, 2, 3, and 5 included three *DoCIPK* genes, chromosomes 4, 6, 7, 9, and 11 included two *DoCIPK* genes, and chromosome 8 included only one *DoCIPK19* gene (Figure 2). There was one chromosome 11 with no *DoCBLs* or *DoCIPKs* that was not shown in this picture. These results indicated that the uneven distributions of *DoCBL* and *DoCIPK* genes on the chromosomes might be related to species evolution and genetic variation.

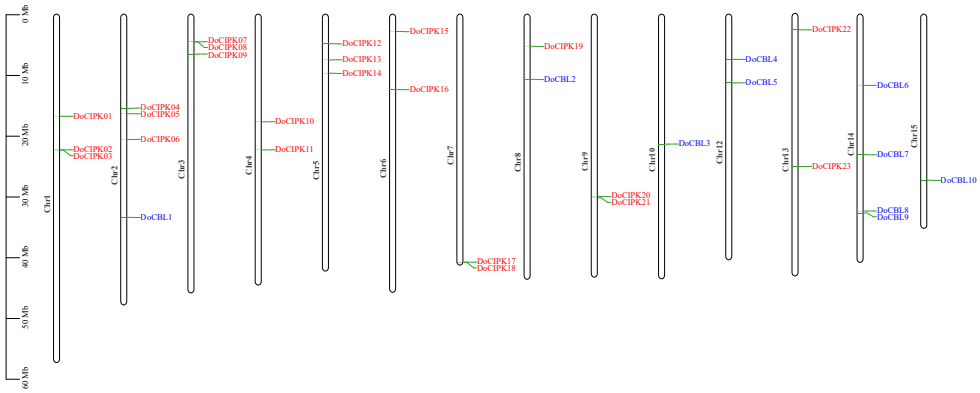

Figure 2. The distribution of *CBL–CIPK* genes on oil persimmon chromosomes. *DoCBL* and *DoCIPK* genes are represented in blue and red, respectively.

Analysis of gene duplication was conducted using MCscanX software. The results showed that four pairs of *DoCBL* genes (80% of the total genes) resulted from segmental duplication, including *DoCBL2* and *DoCBL10* in Group I, *DoCBL4* and *DoCBL7* in Group II, *DoCBL5* and *DoCBL8* in Group III, and *DoCBL3* and *DoCBL6* in Group IV (Figure 3). There were 11 *DoCIPK* gene pairs (69.6% of the total genes) represented within segmental duplication, including 14 *DoCIPKs* in Group I (Intron-less) and two *DoCIPKs* in Group II. Otherwise, only one tandem duplication was found between *DoCIPK07* and *DoCIPK08* (Figure 3, green arc), and their Ka/Ks ratio was 0.18, indicating that they evolved under a purifying selection effect. These findings suggested that the expansion of *DoCBLs* and *DoCIPKs* was mainly due to segmental duplication, which would a play key role in the generation and maintenance of the CBL–CIPK gene family.

2.4. Conserved Motifs and Gene Structure Analysis

To further study the characteristics of DoCBLs and DoCIPKs, the conserved motif distribution and gene structure were investigated. Here, a total of seven motifs were predicted in DoCBL proteins, and four motifs (motifs 1, 2, 3, and 4) existed in all members. Motif 1, 2 and 3 consisted in three EF-hand domains, which had several conserved Asp (D) and Glu (E) amino acid residues (Figure 4b,d). Motif 5 was detected in all DoCBLs except DoCBL7, motif 6 was detected only in members of Group I, and motif 7 existed in members of the other groups, except DoCBL3 and DoCBL7 (Figure 4b). The *DoCBL* genes contained eight to nine exons and seven to eight introns, except *DoCBL7*, suggesting the conservation of exon/intron numbers among CBL family genes (Figure 4c). These results showed that members within close evolutionary relationships had uniform or similar motif compositions and gene structures.

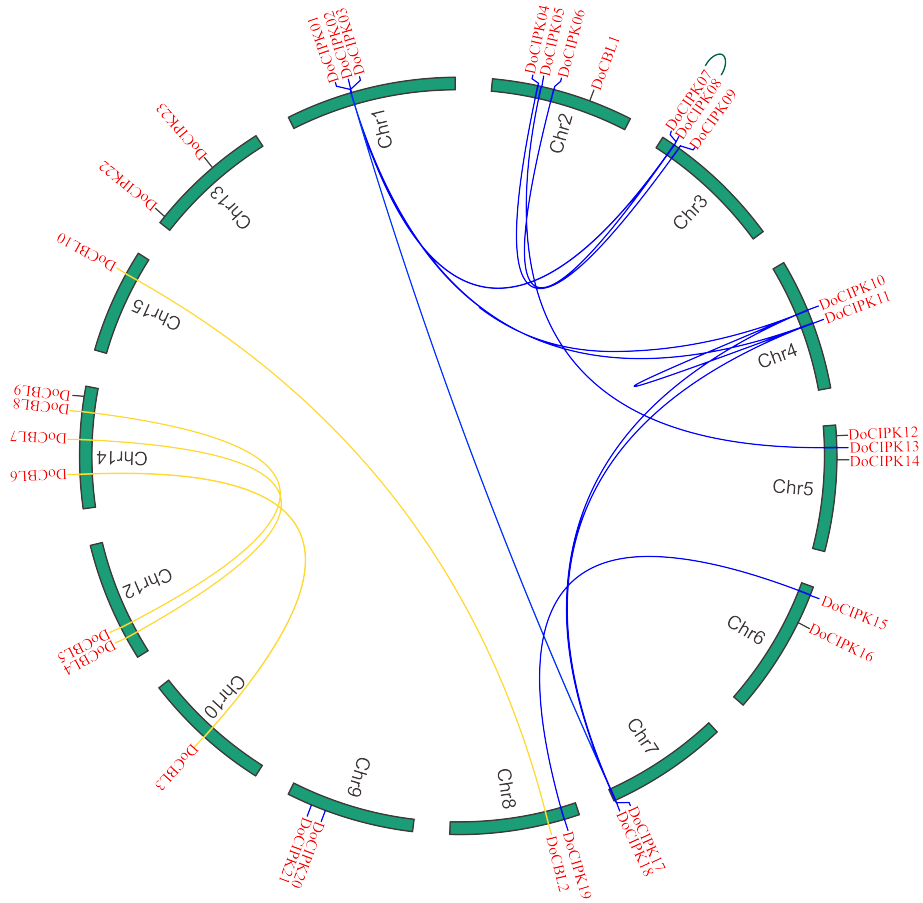

Figure 3. Genome–wide synteny analysis of *CBL–CIPK* genes in oil persimmon. Gene pairs of *DoCBL* and *DoCIPK* genes are linked by blue and yellow lines, respectively. Blue and yellow lines represent segmental duplications, and green arc represents tandem duplications.

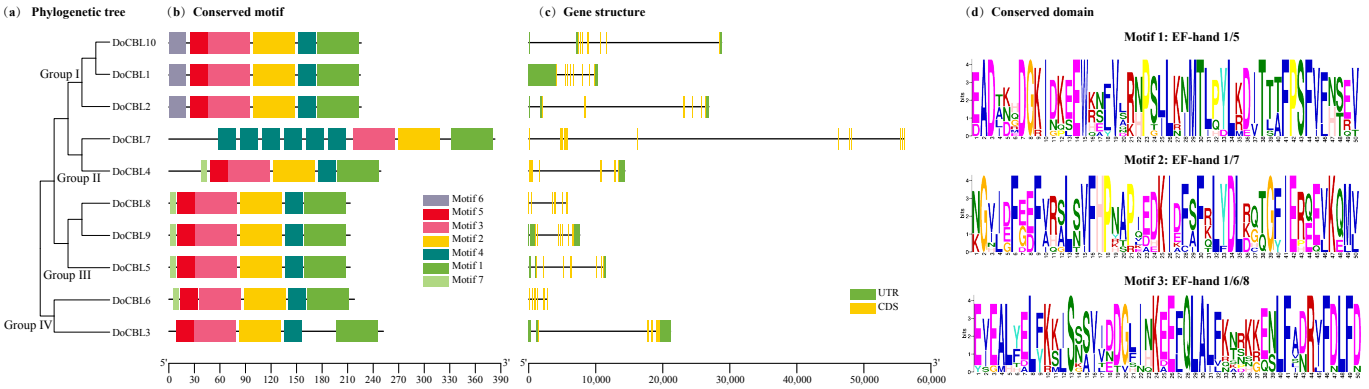

Figure 4. Phylogenetic tree of DoCBL proteins (**a**), motif distribution (**b**), gene structure (**c**) and conserved domains and motifs (**d**).

Fifteen motifs were identified in DoCIPK proteins, and seven motifs (motif 1, 2, 3, 4, 8, 9 and 10) existed in all members, which mainly comprised the NAF domain (motif 8, 9), PPI domain (motif 10, except DoCIPK09), and Ser–Thr kinase domain (motif 1, 2) (Figure 5b,d). Additionally, a strong conservation of the NAF motif was identified in DoCIPKs (Figure 5d), which would be responsible for interacting with DoCBLs. The *DoCIPK* genes of Group I possessed one or two exons and zero or one intron, while *DoCIPK* genes of Group II had 12~15 exons and 11~14 introns (Figure 5c). In general, the exon length and exon/intron

number were moderately conserved between two groups, indicating similar biological functions of *DoCIPKs* in the same group.

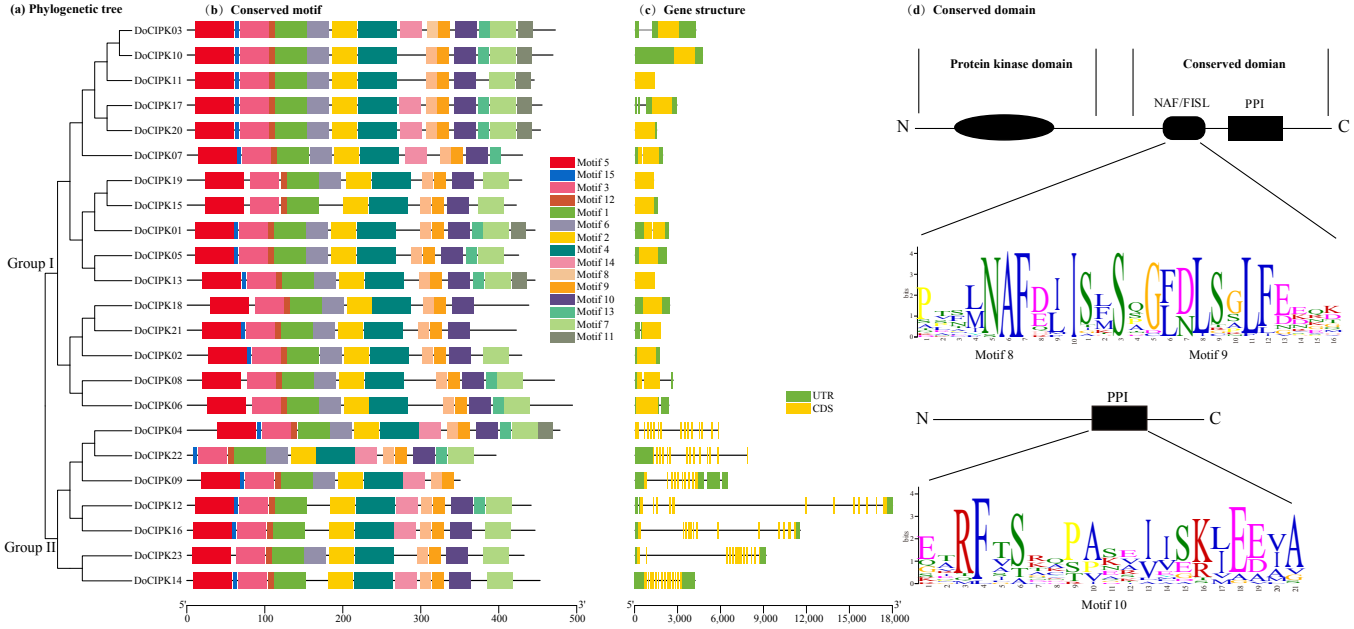

Figure 5. Phylogenetic tree of DoCIPK proteins (**a**), motif distribution (**b**), gene structure (**c**) and conserved domains and motifs (**d**).

2.5. Expression Patterns of DoCBL and DoCIPK Genes by Transcriptome

The expression patterns of *DoCBL* and *DoCIPK* genes in different oil persimmon tissues and at different stages of fruit development and ripening were determined by their transcriptome data. The results showed that the expression of *DoCBLs* and *DoCIPKs* had tissue- and time-specific patterns (Figure 6). *DoCBL1*, *DoCBL2* and *DoCBL5* were highly expressed in fruit, seed, root, stem and leaf. Specifically, *DoCBL2* and *DoCBL4* were highly expressed in fruit, and *DoCBL1* and *DoCBL5* were highly expressed in root and stem (Figure 6a). *DoCBL3*, *DoCBL6*, and *DoCBL7* had lower expression levels in all tissues, while *DoCBL8*, *DoCBL9*, and *DoCBL10* had tissue-specific expression levels (Figure 6a). At different developmental stages of fruit, *DoCBL2*, *DoCBL4*, and *DoCBL5* were highly expressed in six months, while *DoCBL6* and *DoCBL7* were time-specifically expressed, and the other five *DoCBLs* were expressed at low levels in five months, except in May (Figure 6b). Seven *DoCBLs* had higher expression levels in young fruits (in May), and four *DoCBLs* had higher expression levels in mature fruits (in November).

There were eight *DoCIPKs* with high expression levels and four *DoCIPKs* with low expression levels in different tissues, while the other 11 (47.8%) *DoCIPKs* were tissue-specific expressed in oil persimmon (Figure 6c). Five *DoCIPKs* were expressed at low levels, four *DoCIPKs* were highly expressed in different developmental stages of fruit, and 14 (60.9%) *DoCIPKs* had time-specific expression patterns in oil persimmon fruit (Figure 6d). Specifically, some *DoCIPKs* were not only highly expressed in oil persimmon tissues, but also highly expressed at different stages of fruit development and ripening, such as *DoCIPK04*, *DoCIPK05*, *DoCIPK11*, and *DoCIPK15*. In total, the different expression patterns of *DoCBLs* and *DoCIPKs* indicated that they might play different roles in oil persimmon tissue development and fruit growth and ripening.

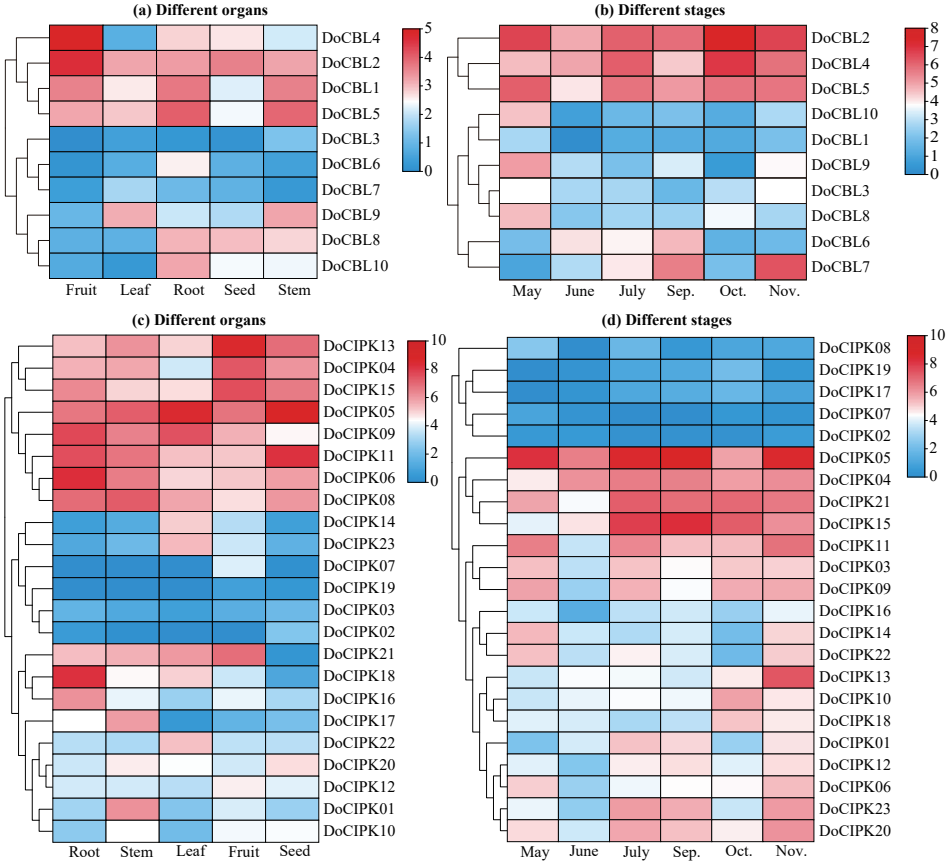

Figure 6. Expression levels of *DoCBL* and *DoCIPK* genes in different oil persimmon tissues (**a**,**c**) and at different stages of oil persimmon fruit development (**b**,**d**), values = Log_2(FPKM + 1).

2.6. Expression Levels of DoCBL and DoCIPK Genes under Different Stresses

We chose the highly and differentially expressed *DoCBL* and *DoCIPK* genes from the aforementioned results to study their responses to abiotic stress and phytohormone stress. The expression levels of seven *DoCBLs* and nine *DoCIPKs* in one-year-old oil persimmon plants were determined under NaCl, drought, ABA, and $Ca(NO_3)_2$ stress. The primers for these genes are shown in Supplement Table S1. As shown in Figure 7, there were four *DoCBLs* (*DoCBL2*, *DoCBL4*, *DoCBL5* and *DoCBL8*) and four *DoCIPKs* (*DoCIPK05*, *DoCIPK09*, *DoCIPK11* and *DoCIPK15*) up-regulated under NaCl stress, and the other genes had no significant changes when compared to controls. Most of them had higher expression levels under 150 mM NaCl stress than under 300 mM NaCl stress ($p < 0.05$). Similarly, five *DoCBLs* (*DoCBL1*, *DoCBL2*, *DoCBL5*, *DoCBL8* and *DoCBL9*) were up-regulated under drought stress, especially after 15 days without watering ($p < 0.05$). Five *DoCIPKs* (*DoCIPK04*, *DoCIPK05*, *DoCIPK09*, *DoCIPK15* and *DoCIPK21*) were up-regulated after seven or 15 days without watering ($p < 0.05$). In contrast, five *DoCBLs* (*DoCBL2*, *DoCBL5*, *DoCBL7*, *DoCBL8* and *DoCBL9*) and four *DoCIPKs* (*DoCIPK04*, *DoCIPK06*, *DoCIPK11* and *DoCIPK15*) were significantly down-regulated in oil persimmon leaves under 100 μM ABA stress ($p < 0.05$), while *DoCIPK13* and *DoCIPK21* were up-regulated under 50 μM ABA compared to controls (Figure 7). Four *DoCBLs* (*DoCBL5*, *DoCBL7*, *DoCBL8* and *DoCBL9*) and two *DoCIPKs* (*DoCIPK05* and *DoCIPK09*) were significantly up-regulated under 6 mM $Ca(NO_3)_2$ stress ($p < 0.05$), and the other genes (except for *DoCBL2*) had no significant changes compared to controls (Figure 7). In conclusion, the expression patterns of these genes were similar under NaCl, drought, and $Ca(NO_3)_2$ stress but different under ABA stress. For instance, *DoCBL5*, *DoCBL8*, *DoCBL9*, *DoCIPK05*, *DoCIPK09*, and *DoCIPK15* were up-regulated by NaCl, drought, and $Ca(NO_3)_2$ stress, but they were down-regulated or unchanged under ABA stress.

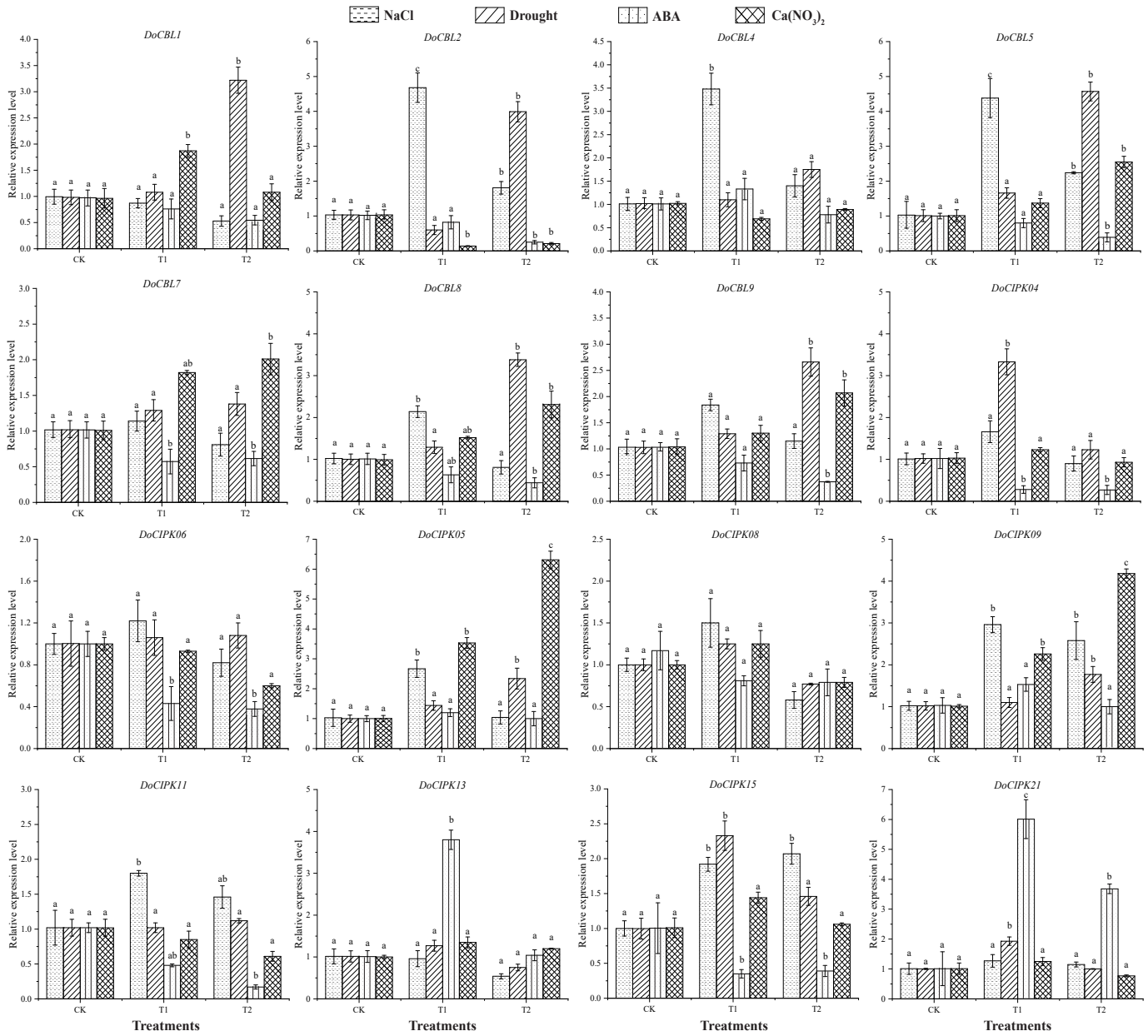

Figure 7. Expression levels of *DoCBL* and *DoCIPK* genes under NaCl, drought, ABA and $Ca(NO_3)_2$ stress. NaCl: T1 = 150 mM and T2 = 300 mM; drought: T1 = 7 d and T2 = 15 d; ABA: T1 = 50 μM and T2 = 100 μM; $Ca(NO_3)_2$: T1 = 2 mM and T2 = 6 mM. Bars with different letters within each panel are significant differences at $p < 0.05$ among different concentrations of each stress according to Tukey's test.

2.7. Gene Cloning and Subcellular Localization of DoCBL5 and DoCIPK05

We chose *DoCBL5* and *DoCIPK05* as typical genes to study their interaction and function. The full-length coding sequences of *DoCBL5* and *DoCIPK05* were cloned. The coding regions of *DoCBL5* and *DoCIPK05* were obtained by sequencing, and they were 642 bp and 1278 bp, encoding 213 and 425 amino acids, respectively. The results of sequence alignment showed that the cloned sequence of *DoCBL5* had one base different from the reference sequence, while *DoCIPK05* had four bases different from the reference sequence (Supplement Figure S1), which would contribute to correcting the reference genome sequences of oil persimmon. To verify the above results, we transiently expressed p35S–DoCBL5–GFP and p35S–DoCIPK05–GFP fusion proteins in tobacco leaves. The

results showed that DoCBL5 and DoCIPK05 were both located in the plasma membrane of tobacco leaf cells (Figure 8). It was speculated that DoCBL5 and DoCIPK05 might be involved in transmembrane transport and signal transduction pathway.

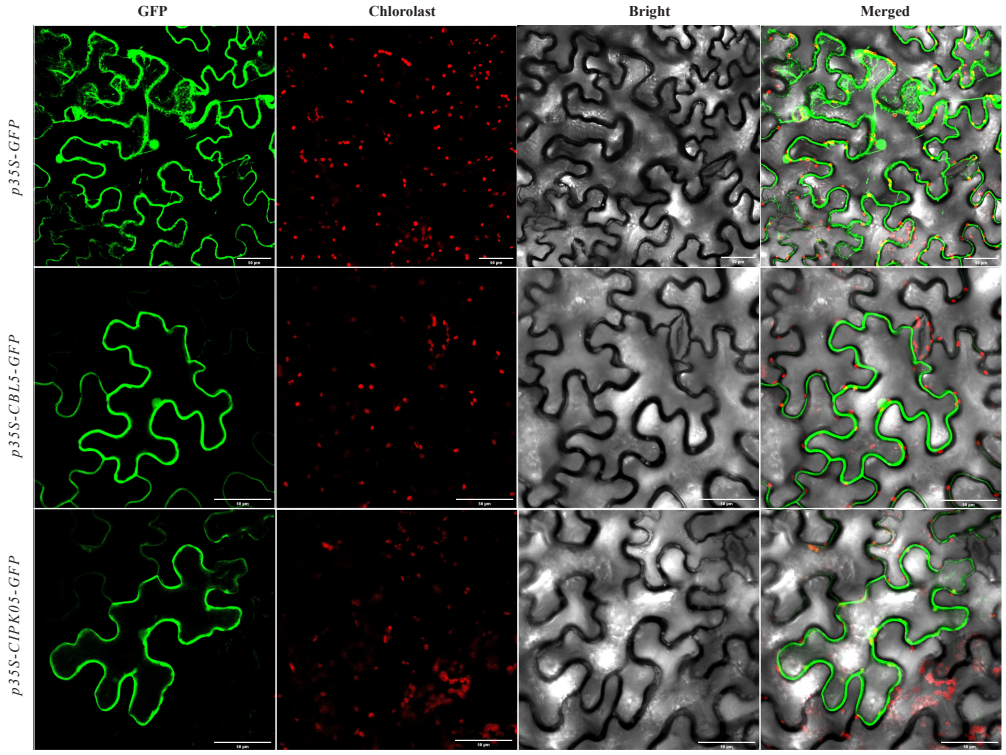

Figure 8. Subcellular localization of the p35S–DoCBL5–GFP and p35S–DoCIPK05–GFP fusion proteins in tobacco leaves. Free GFP served as a control. Bars = 50 μm.

2.8. The Interaction Network of DoCBL5 and DoCIPK05

The protein interaction network of DoCBL5 and DoCIPK05 was analyzed by String software to determine the potential functions and signal transduction pathways. The results showed that the regulatory network of DoCBL5, a homolog of AtCBL1, mainly interacted with CIPK and AKT1 proteins to regulate Ca^{2+} signals and K^+ homeostasis (Figure 9a). DoCIPK05, a homolog of AtCIPK6/AtSIP3, interacted with CBL, AKT1, PP2C and SNF, which affected the activity of AKT1, PP2C and SNF to regulate K^+ and ABA homeostasis in cells (Figure 9b). DoCBL5 interacted with DoCIPK05, and the DoCBL5–DoCIPK05 complex might be involved in Ca^{2+}-related and ABA signal transduction pathway under abiotic stresses.

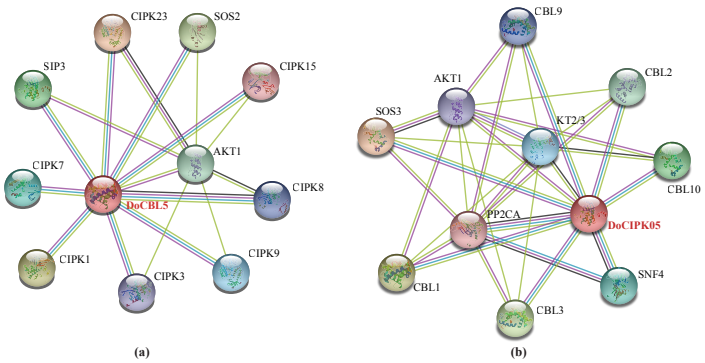

Figure 9. Protein–protein interaction network of DoCBL5 protein (**a**) and DoCIPK05 protein (**b**).

3. Discussion

In plants, the CBL–CIPK gene family comprises a plant-specific module for decoding Ca^{2+} signals during plant growth and responses to various abiotic stresses. Due to the availability of fully sequenced genomes, the CBL–CIPK gene family has been reported in several plant species. However, information about oil persimmon CBL–CIPK genes remains elusive. Here, a total of ten *DoCBL* genes and 23 *DoCIPK* genes were identified and systematically characterized in oil persimmon.

DoCBL proteins contained three conserved EF-hand domains consisting of motif 1, 2, and 3, respectively (Figure 4). However, other CBL proteins were previously reported to contain four EF-hands [5,16,28]. According to the reports of Mohanta et al. [6], CBL proteins should contain three calcium-binding EF-hands, not four or incomplete four. It was due to the fact that incomplete and nonfunctional EF-hands could not be transferred for millions of years in the process of evolution [6]. Each EF-hand contained several conserved Asp (D) and Glu (E) amino acid residues (Figure 4d), which were conferred on binding to Ca^{2+} [29]. The phylogenetic tree showed that DoCBLs were clustered into four groups, consistent with the similar presence of conserved Gly and Cys residues on their N-termini. Similar results have also been found in Arabidopsis [30], grapevine [28], pineapple (*Ananas comosus*) [31] and apple [32]. The Gly and Cys sites play roles in signal transduction, protein–protein interactions and protein–membrane attachment [33,34]. DoCBL5, DoCBL8, and DoCBL9 contain conserved MGCXXS/T motifs with Gly and Cys residues in their N-termini, which contribute to the anchorage of CBLs in the membrane to transduce Ca^{2+} signals [32]. In addition, the conserved motif analysis along with the phylogenetic tree showed that *DoCBL* genes with similar motifs were clustered into the same group (Figure 4c). The structural diversification among the different groups might allow different *DoCBL* genes to function differently in oil persimmon [35].

The conserved NAF domain, a 24-amino acid motif, is specific and necessary to mediate the interaction between CBL and CIPK in plants. After sensing and decoding Ca^{2+} signals, CBLs interact with the NAF/FISL motifs at the C-terminus of CIPKs to activate them, and then the activated CIPKs participate in Ca^{2+} signal transduction by phosphorylating target proteins [5]. Sequence analysis showed that Ser–Thr kinase, NAF, and PPI domains were identified in 22 DoCIPK genes, except for DoCIPK09 (Table 1), which were similar to CIPK proteins in Arabidopsis and Populus [36]. The phylogenetic tree of DoCIPKs was divided into two groups: intron-less and intron-rich, with a great difference in intron numbers between them. Similar results have also been found in Arabidopsis [37], apple [22] and grapevine [28]. The exon length and exon/intron number of *DoCIPK* genes were moderately conserved between two groups (Figure 5c), indicating that they might have a same biological function in the same group. In addition, the distribution of the *CBL* and *CIPK* genes in the chromosomes was uneven, which might be related to species evolution and genetic variation [22]. Synteny analysis of CBL–CIPK gene family showed gene expansion that was mainly attributed to segmental duplication, in which multiple genes undergo polyploidy followed by chromosome rearrangements [38]. In conclusion, these findings suggested that CBL–CIPK family genes in oil persimmon were relatively conserved in structure during evolution, which also indicated the functional conservation of decoding Ca^{2+} signals [39].

The diversity and specificity of the expression patterns of *CBL–CIPK* genes may play important roles in unraveling their biological function in signal transduction [2,29]. In this study, the differential expression patterns of *CBL–CIPK* genes were determined in different oil persimmon tissues and at various stages of fruit development and ripening. The results showed that the expression patterns of *DoCBLs* and *DoCIPKs* were tissue- and time-specific (Figure 6), which suggested the distinct effect of *CBL–CIPK* genes. *DoCBL1*, *DoCBL2* and *DoCBL5* were strongly expressed in fruit, seed, root, stem and leaf, while *DoCBL3*, *DoCBL6* and *DoCBL7* were expressed at low levels in all five tissues (Figure 6a). These results suggested their potential functions in oil persimmon genetic transformation. Higher expression levels of *DoCBL2*, *DoCBL4* and *DoCBL5* were found at different stages in

fruit development, indicating their special roles in fruit development [35]. Some *DoCIPKs* were highly expressed in fruit, seed, root, stem, and leaf, as well as at different development stages of fruit, such as *DoCIPK04*, *DoCIPK05*, *DoCIPK09*, *DoCIPK11* and *DoCIPK15*. In contrast, *DoCIPK02*, *DoCIPK07* and *DoCIPK19* were suppressed in all tissues and at all stages of fruit development. The tissue- and time-specific expression patterns of *DoCIPKs* indicated that they might have various functions in oil persimmon growth and fruit development [31].

Interestingly, the expression of *CBL–CIPK* genes was induced by many factors, such as biotic and abiotic stresses and phytohormones [37,40]. Therefore, we selected seven *DoCBLs* and nine *DoCIPKs* to investigate their expression patterns under different stress conditions. The expression patterns of the analyzed *DoCBLs* and *DoCIPKs* were different among the different stresses. For example, *DoCBL5*, *DoCBL8*, *DoCIPK05* and *DoCIPK09* were significantly up-regulated under NaCl (150 mM), drought (15 days), and $Ca(NO_3)_2$ (60 mM) treatments, but they were suppressed or unchanged under ABA stress ($p < 0.05$). Among these four stresses, drought treatment resulted in the largest number of up-regulated genes, and ABA treatment resulted in the largest number of down-regulated genes in oil persimmon leaves (Figure 7). These results were similar to *TaCBL9* and *TaCIPK24* of wheat under different stresses [21]. In brief, the expression patterns of the assayed genes differed among the various treatments, indicating that *DoCBLs* and *DoCIPKs* might play different roles in responding to various stresses [19].

The CBL–CIPK network is currently thought to be a major regulator in ion homeostasis [41]. Each CBL interacts with several CIPKs, but each CIPK interacts with one or more CBLs. The full-length coding sequences of *DoCBL5* (a homolog of AtCBL1) and *DoCIPK05* (a homolog of AtCIPK6/AtSIP3) were cloned. By transiently expressing 35S–DoCBL5–GFP and 35S–DoCIPK05–GFP fusion proteins in tobacco leaves, DoCBL5 and DoCIPK05 were found to be located in the plasma membrane (Figure 8). In *Brassica napus*, BnCIPK6 was mainly localized in the plasma membrane and nucleus, whereas its interaction partner BnCBL1 was localized on the plasma membrane [42]. In addition, previous reports revealed that most CIPK proteins expressed as GFP fusions exhibited cytoplasmic and/or nuclear localization due to the absence of recognizable localization signals [7,8], while CBLs could target CIPKs to the plasma membrane or vacuolar membrane [7,43]. The different cellular locations of CBL–CIPK complexes direct their distinct functions. AtCIPK1 and AtCIPK23 are recruited to the plasma membrane by interaction with AtCBL1 and AtCBL9, which localize to the plasma membrane [44]. In this study, the protein interaction network of DoCBL5 and DoCIPK05 showed that they interacted with each other, and they also interacted with AKT1, PP2C and SNF to regulate the Ca^{2+} signals, K^+ and ABA homeostasis in cells (Figure 9).Similarly, AtCBL1 and AtCIPK6 have been shown to activate the AKT1 channel through the CBL–CIPK–PP2CA network [40,44]. These results suggest that DoCBL5–DoCIPK05 may functionally interact with each other during their involvement in the Ca^{2+}-related and ABA signal transduction pathways [45]. Further study of the *CBL–CIPK* gene family will be crucial for a better understanding of their role in signal transduction and stress responses.

4. Materials and Methods

4.1. Identification of CBL–CIPK Gene Family in Oil Persimmon

An EF-hand calcium-binding domain (PS50222) and an HMM profile of the NAF domain (PF03822) were employed to identify the putative DoCBL and DoCIPK proteins from oil persimmon genome sequences using the software HMMER ver. 3.3.2 [46] with a cutoff E-value of $\leq 1 \times 10^{-10}$ [47]. Subsequently, the candidates were manually curated, and the nonredundant CBL and CIPK proteins were further analyzed using the NCBI Conserved Domain Database (CDD, http://www.ncbi.nlm.nih.gov/cdd/ (accessed on 16 December 2022)) and SMART programs (http://smart.embl--heidelberg.de/ (accessed on 16 December 2022)) to confirm the presence of EF-hand domain and NAF domain, respectively. The theoretical isoelectric point (pI) and molecular weight (Mw) of the DoCBL

and DoCIPK proteins were predicted using the Prot–Param tool (http://web.expasy.org/protparam/ (accessed on 16 December 2022)).

4.2. Phylogenetic Analysis of CBL–CIPK Gene Family

All of the putative CBL–CIPK proteins were aligned using MUSCLE v. 3.8.31 [48] with the 'auto' setting. The representative phylogenetic trees of CBL and CIPK were constructed based on proteins from six eudicots, including *Diospyros oleifera*, *Arabidopsis thaliana*, *Actinidia chinensis*, *Malus domestica*, *Solanum lycopersicum*, and *Vitis vinifera*. AtCBL and AtCIPK proteins were obtained from the Arabidopsis Information Resource (TAIR) (http://www.arabidopsis.org/ (accessed on 16 December 2022)). The other candidates of four species were identified using the aforementioned method. To improve the valid phylogeny signals, the low-quality alignment regions and incorrect sequences with apparent splice variants were removed from the list (Supplement Table S1) [49]. Finally, the conserved blocks were retained by Gblocks ver. 0.91b [15], and then the maximum likelihood (ML) trees were preformed using iQ–TREE v. 2 [50] with the LG + R6 model, 1000 bootstraps, and the Shimodaira–Hasegawa-like aLRT (SH–aLRT) test. Putative functional homologs were identified from a gene group that contained the query genes from Arabidopsis, which was likely derived from an ancestral gene from dicots [51].

4.3. Chromosomal Location, Gene Duplication, Gene Structure and Conserved Motifs

The software TBtools v. 1.098761 [52] was used to locate and mark the physical distribution of the *DoCBL* and *DoCIPK* genes on the oil persimmon chromosomes. Genome–wide synteny analysis was conducted using MCscanX software [53]. Gene duplication and the gene structure of *DoCBLs* and *DoCIPKs* were shown by TBtools [52]. The conserved motifs of all DoCBL and DoCIPK proteins were predicted by the online MEME tool (http://meme--suite.org/tools/meme (accessed on 16 December 2022)). The maximum number of motifs was set to 7 and 15, respectively, and the optimum motif width was $\geq$6 and $\leq$50.

4.4. Plant Materials and Growth Conditions

One-year-old oil persimmon grafted seedlings were used to conduct experiments under different stresses in a greenhouse with a natural temperature and humidity. A total of 60 pots (one plant per plot) were arranged in 5 completely randomized groups, and each group was assigned to one treatment, including control (CK), NaCl, ABA, $Ca(NO_3)_2$ and drought. All plants were fertigated with half-strength Hoagland's solution [54] at the beginning of experiment. Three treatments were performed with NaCl (T1 = 150 mM and T2 = 300 mM), ABA (T1 = 50 μM and T2 = 100 μM) and $Ca(NO_3)_2$ (T1 = 2 mM and T2 = 6 mM) solution once a week for 4 weeks. The controls were watered once a week, and drought treatment was performed without water for 7 days (T1) and 15 days (T2). Finally, we harvested leaves from each plant, and every 2 pots were designed as biological replicates.

4.5. Expression Patterns of DoCBL and DoCIPK Genes

To investigate the expression patterns of *DoCBL* and *DoCIPK* genes in different tissues, the published transcriptome data of oil persimmon were downloaded from NCBI (PRJNA562975) [27]. Additionally, we determined the expression patterns of these genes at different stages of fruit development by RNA = Seq (data not published). First, all RNA-Seq data were qualitatively controlled by fastp, and then the gene expression was further calculated and analyzed with clean reads. The expression levels of *DoCBL* and *DoCIPK* genes were obtained with FPKM (fragments per kilobase of exon per million fragments mapped) values. Finally, thermal maps of *DoCBL* and *DoCIPK* genes were drawn with $\log_2$(FPKM + 1) values using TBtools.

The expression levels of *DoCBLs* and *DoCIPKs* under different stresses were determined by quantitative real-time PCR (qRT–PCR). Total RNA was extracted from fresh root and leaf samples using the BioTeke plant total RNA extraction kit (BioTeke Corporation,

Beijing, China) according to the manufacturer's instructions. The cDNA templates were prepared using a reverse transcription HiScript 1st Strand cDNA Synthesis Kit (Vazyme Bio Tech Co., Ltd., Beijing, China). The primers of 15 genes were designed with the open reading frame and its 3′ or 5′ untranslated region of each gene using the NCBI primer-BLAST tool (Supplement Table S2). The specificity of primers was confirmed by PCR amplification. Real-time RT-PCR (qRT-PCR) was carried out using a 7500 Fast Real–Time PCR system (Applied Biosystems, Waltham, CA, USA) with three technical replicates for each cDNA sample. Each reaction was in a final volume of 20 μL, containing 10 μL of TB Green *Premix Ex Taq*, 0.4 μL of ROX Reference Dye II, 0.8 μL of upstream and downstream primers, 1 μL of cDNA template and 7 μL of ddH_2O. The PCR thermal cycler was set as follows: predenaturation at 95 °C for 30 s; 40 cycles of 95 °C for 5 s and 60 °C for 34 s; the dissociation stage was set as follows: 95 °C for 15 s, 60 °C for 60 s and 95 °C for 15 s. The housekeeping gene *Dkactin* (GenBank No. AB473616) was chosen as the internal control, and the relative expression was quantitatively analyzed by the $2^{-\Delta\Delta Ct}$ method [55].

4.6. Gene Cloning and Subcellular Localization

To verify the true location of the DoCBL5 and DoCIPK05 proteins, a GFP fusion protein in tobacco leaves was expressed and detected. First, a high-fidelity PCR was carried out to obtain the full-length coding sequences (CDSs) of *DoCBL5* and *DoCIPK05*. The reaction conditions were as follows: first 95 °C for 15 s; then 55 °C for 15 s, 72 °C for 30 s, and 39 cycles; last 72 °C for 5 min. The PCR products were separated by 1% agarose gel electrophoresis, and the fragment was recovered by gel cutting. Second, the amplified target fragments were cloned into the p35S–K–GFP vector (supplied by Shanghai Swift Tide Technology Development Co., Ltd., Shanghai, China) by the Golden Gate reaction with the BsaI–HFv2 restriction enzyme (New England Biolabs) [56]. Primers for the restriction sites at both ends of the target gene were designed on NCBI (Supplement Table S2). Then, the recombinant plasmid was transformed into competent *E. coli* DH5α and sequenced to verify the fidelity of the PCR product. The constructs p35S–DoCBL5–GFP and p35S–DoCIPK05–GFP were transformed into *Agrobacterium tumefaciens* (strain GV3101) with three biological replicates via cold shock. Finally, GV3101 harboring the combined constructs and control vector was infiltrated into tobacco (*Nicotiana benthamiana*) leaves. After 48 h, fluorescence images were captured using an FV1000 confocal laser-scanning microscope (Olympus Corporation, Tokyo, Japan).

4.7. Data Analysis

All qRT–PCR data were analyzed with one-way ANOVA, and multiple comparisons were evaluated with Tukey's test ($p < 0.05$) using SPSS v. 19.0 (SPSS Inc., Chicago, IL, USA) based on the values of three complete randomized replicates. The histograms were generated using OriginPro 2018 (OriginLab, Northampton, MA, USA).

5. Conclusions

Our research investigated the characteristics of the CBL–CIPK gene family in oil persimmon via phylogenetic, evolution and structural analysis. The phylogenetic trees were constructed with the CBL–CIPK protein sequences of six dicot plants successfully. The tree of DoCBLs were clustered into four groups with distant motifs and specific sites in their N-terminus. Moreover, DoCIPKs were divided into intron-rich and intron-less groups with distant exons numbers. The expression profiles of *CBL–CIPK* genes were also determined in different oil persimmon tissues and at various stages of fruit development, as well as in the response to stresses. PPI network analysis results showed that DoCBL5 and DoCIPK05 were hypothesized to interact with AKT1, PP2C, and SNF to regulate the Ca^{2+} signals, K^+, and ABA homeostasis in cells. The theoretical foundation was established in the present study for the further functional characteristics of the CBL–CIPK gene families in oil persimmon. However, more work is needed to decipher the interaction networks

between DoCBLs and DoCIPKs, as well as the responsive patterns of CBL–CIPK genes to various stresses.

Supplementary Materials: The following supporting information can be downloaded at: https://www.mdpi.com/article/10.3390/horticulturae9010030/s1, Figure S1: PCR amplification and sequence alignment of *DoCBL5* (a) and *DoCIPK05* (b); Table S1: List of CBL–CIPK proteins used for constructing the phylogenetic tree; Table S2. Primers used in qRT-PCR analysis and gene cloning for *DoCBLs* and *DoCIPKs*.

Author Contributions: Conceptualization, C.L., B.G., and Y.X.; methodology, Y.W.; formal analysis, C.L. and Y.W.; investigation, J.Y. and G.T.; resources, J.Y.; writing—original draft preparation, C.L.; writing—review and editing, X.Y. and K.W.; supervision, B.G. and Y.X.; project administration, B.G.; funding acquisition, Y.X. All authors have read and agreed to the published version of the manuscript.

Funding: This research was funded by the National Key R & D Program of China (grant No. 2019YFD1000600 and 2018YFD1000606), and the Key Agricultural New Varieties Breeding Projects of the Zhejiang Province Science and Technology Department (grant No. 2021C02066–10).

Data Availability Statement: Not applicable.

Conflicts of Interest: The authors declare no conflict of interests.

References

1. Riveras, E.; Alvarez, J.M.; Vidal, E.A.; Oses, C.; Vega, A.; Gutiérrez, R.A. The calcium ion Is a second messenger in the nitrate signaling pathway of Arabidopsis. *Plant Physiol.* **2015**, *169*, 1397–1404. [CrossRef] [PubMed]
2. Sheng, L. The CBL-CIPK network in plant calcium signaling. *Trends Plant Sci.* **2009**, *14*, 37–42.
3. Petit-Glatron, M.F.; Grajcar, L.; Munz, A.; Chambert, R. The contribution of the cell wall to a transmembrane calcium gradient could play a key role in Bacillus subtilis protein secretion. *Mol. Microbiol.* **2010**, *9*, 1097–1106. [CrossRef] [PubMed]
4. Sharma, A.; Shankhdhar, D.; Shankhdhar, S.C. The role of calcium in plant signal transduction under macronutrient deficiency stress. In *Plant Macronutrient Use Efficiency*; Sharma, A., Shankhdhar, D., Shankhdhar, S.C., Eds.; Elsevier: Amsterdam, The Netherlands, 2017; pp. 181–196.
5. Sanyal, S.K.; Pandey, A.; Pandey, G.K. The CBL–CIPK signaling module in plants: A mechanistic perspective. *Physiol. Plant* **2015**, *155*, 89–108. [CrossRef]
6. Mohanta, T.K.; Mohanta, N.; Mohanta, Y.K.; Parida, P.; Bae, H. Genome-wide identification of calcineurin b-Like (CBL) gene family of plants reveals novel conserved motifs and evolutionary aspects in calcium signaling events. *BMC Plant Biol.* **2015**, *15*, 189. [CrossRef]
7. Batistic, O.; Sorek, N.; Schültke, S.; Kudla, S.Y. Dual fatty acyl modification determines the localization and plasma membrane targeting of CBL/CIPK Ca^{2+} signaling complexes in Arabidopsis. *Plant Cell* **2008**, *20*, 1346–1362. [CrossRef]
8. de la Torre, F.; Gutiérrez-Beltrán, E.; Pareja-Jaime, Y.; Chakravarthy, S.; Martin, G.B.; del Pozoa, O. The tomato calcium sensor CBL10 and its interacting protein kinase CIPK6 define a signaling pathway in plant immunity. *Plant Cell* **2013**, *25*, 2748–2764. [CrossRef]
9. Albrecht, V.; Ritz, O.; Linder, S.; Harter, K.; Kudla, J. The NAF domain defines a novel protein–protein interaction module conserved in Ca^{2+}-regulated kinases. *EMBO J.* **2001**, *20*, 1051–1063. [CrossRef]
10. Ohta, M.; Guo, Y.; Halfter, U.; Zhu, J.K. A novel domain in the protein kinase SOS2 mediates interaction with the protein phosphatase 2C ABI2. *Proc. Natl. Acad. Sci. USA* **2003**, *100*, 11771–11776. [CrossRef]
11. Ji, H.T.; Pardo, J.M.; Batelli, G.; Van Oosten, M.J.; Bressan, R.A.; Li, X. The salt overly sensitive (SOS) pathway: Established and emerging roles. *Mol. Plant* **2013**, *6*, 275–286. [CrossRef]
12. Yin, X.; Xia, Y.; Xie, Q.; Cao, Y.; Wang, Z.; Hao, G.; Song, J.; Zhou, Y.; Jiang, X. The protein kinase complex CBL10–CIPK8–SOS1 functions in Arabidopsis to regulate salt tolerance. *J. Exp. Bot.* **2019**, *6*, 1801–1814. [CrossRef] [PubMed]
13. Batistic, O.; Kudla, J. Integration and channeling of calcium signaling through the CBL calcium sensor/CIPK protein kinase network. *Planta* **2004**, *219*, 915–924. [CrossRef] [PubMed]
14. Yang, Y.; Zhang, C.; Tang, R.J.; Xu, H.X.; Luan, S. Calcineurin B-Like proteins CBL4 and CBL10 mediate two independent salt tolerance pathways in Arabidopsis. *Int. J. Mol. Sci.* **2019**, *20*, 2421. [CrossRef] [PubMed]
15. Castresana, J. Selection of conserved blocks from multiple alignments for their use in phylogenetic analysis. *Mol. Biol. Evol.* **2000**, *17*, 540–552. [CrossRef]
16. Kolukisaoglu, U.; Weinl, S.; Blazevic, D.; Batistic, O.; Kudla, J. Calcium sensors and their Interacting protein kinases: Genomics of the Arabidopsis and rice CBL-CIPK signaling networks. *Plant Physiol.* **2004**, *134*, 43–58. [CrossRef]
17. Cuéllar, T.; Azeem, F.; Andrianteranagna, M.; Pascaud, F.; Verdeil, J.-L.; Sentenac, H.; Zimmermann, S.; Gaillard, I. Potassium transport in developing fleshy fruits: The grapevine inward K^+ channel VvK1.2 is activated by CIPK-CBL complexes and induced in ripening berry flesh cells. *Plant J.* **2013**, *73*, 1006–1018. [CrossRef] [PubMed]

18. Kanwar, P.; Sanyal, S.K.; Tokas, I.; Yadav, A.K.; Pandey, A.; Kapoor, S.; Pandey, G.K. Comprehensive structural, interaction and expression analysis of CBL and CIPK complement during abiotic stresses and development in rice. *Cell Calcium* **2014**, *56*, 81–95. [CrossRef] [PubMed]
19. Mao, J.J.; Manik, S.M.N.; Shi, S.J.; Chao, J.T.; Jin, Y.R.; Wang, Q.; Liu, H.B. Mechanisms and physiological roles of the CBL-CIPK networking system in *Arabidopsis thaliana*. *Genes* **2016**, *7*, 62. [CrossRef]
20. Xiang, Y.; Huang, Y.M.; Xiong, L.Z. Characterization of stress-responsive *CIPK* genes in rice for stress tolerance improvement. *Plant Physiol.* **2007**, *144*, 1416. [CrossRef]
21. Tao, S.; Yan, W.; Meng, W.; Li, T.; Yi, Z.; Wang, X.; Wei, S.; He, G.; Yang, G. Identification and comprehensive analyses of the *CBL* and *CIPK* gene families in wheat (*Triticum aestivum* L.). *BMC Plant Biol.* **2015**, *15*, 265.
22. Niu, L.L.; Dong, B.Y.; Song, Z.H.; Dong, M.; Fu, Y.J. Genome-wide identification and characterization of CIPK family and analysis responses to various stresses in apple (*Malus domestica*). *Int. J. Mol. Sci.* **2018**, *19*, 2131. [CrossRef] [PubMed]
23. Tang, J.; Jing, L.; Hui, L.; Li, X.; Yang, Q.; Cheng, Z.M.; Chang, Y. Characterization of CIPK family in asian pear (*Pyrus bretschneideri* Rehd) and co-expression analysis related to salt and osmotic stress responses. *Front. Plant Sci.* **2016**, *7*, 1361. [CrossRef] [PubMed]
24. Duangjai, S.; Wallnfer, B.; Samuel, R.; Munzinger, J.; Chase, M.W. Generic delimitation and relationships in Ebenaceae sensu lato: Evidence from six plastid DNA regions. *Am. J. Bot.* **2006**, *93*, 1808–1827. [CrossRef] [PubMed]
25. Woolf, A.B.; Ben-Arie, R. Persimmon (*Diospyros kaki* L.). In *Postharvest Biology and Technology of Tropical and Subtropical Fruits*; Yahia, E.M., Ed.; Woodhead Publishing: Cambridge, UK, 2011; Volume 4, pp. 166–193, 194e.
26. Suo, Y.; Sun, P.; Cheng, H.; Han, W.; Fu, J. A high-quality chromosomal genome assembly of *Diospyros oleifera* Cheng. *GigaScience* **2020**, *9*, giz164. [CrossRef]
27. Zhu, Q.G.; Xu, Y.; Yang, Y.; Guan, C.F.; Zhang, Q.Y.; Huang, J.W.; Grierson, D.; Chen, K.S.; Gong, B.C.; Yin, X.R. The persimmon (*Diospyros oleifera* Cheng) genome provides new insights into the inheritance of astringency and ancestral evolution. *Hortic. Res.* **2019**, *6*, 138. [CrossRef]
28. Yue, X.; Liu, J.; Dong, C.; Cheng, Z.M. The CBL and CIPK gene family in grapevine (*Vitis vinifera*): Genome-wide analysis and expression profiles in response to various abiotic stresses. *Front. Plant Sci.* **2017**, *8*, 978.
29. Tang, R.J.; Wang, C.; Li, K.; Luan, S. The CBL–CIPK calcium signaling network: Unified paradigm from 20 years of discoveries. *Trends Plant Sci.* **2020**, *25*, 604–617. [CrossRef]
30. Kleist, T.J.; Spencley, A.L.; Luan, S. Comparative phylogenomics of the CBL-CIPK calcium-decoding network in the moss Physcomitrella, Arabidopsis, and other green lineages. *Front. Plant Sci.* **2014**, *5*, 187. [CrossRef]
31. Aslam, M.; Fakher, B.; Jakada, B.H.; Zhao, L.; Cao, S.; Cheng, Y.; Qin, Y. Genome-wide identification and expression profiling of CBL-CIPK gene family in pineapple (*Ananas comosus*) and the role of *AcCBL1* in abiotic and biotic stress response. *Biomolecules* **2019**, *9*, 293. [CrossRef]
32. Chen, P.H.; Yang, J.; Mei, Q.L.; Liu, H.Y.; Cheng, Y.P.; Ma, F.W.; Mao, K. Genome-wide analysis of the apple CBL family reveals that Mdcbl10.1 functions positively in modulating apple salt tolerance. *Int. J. Mol. Sci.* **2021**, *22*, 12430. [CrossRef]
33. Linder, M.E.; Deschenes, R.J. Palmitoylation: Policing protein stability and traffic. *Nat. Rev. Mol. Cell Biol.* **2007**, *8*, 74–84. [CrossRef] [PubMed]
34. Smotrys, J.E.; Linder, M.E. Palmitoylation of intracellular signaling proteins: Regulation and function. *Annu. Rev. Biochem.* **2004**, *73*, 559–587. [CrossRef] [PubMed]
35. Yin, X.; Wang, Q.L.; Chen, Q.; Xiang, N.; Yang, Y.Q.; Yang, Y.P. Genome-wide identification and functional analysis of the calcineurin b-like protein and calcineurin b-like protein-interacting protein kinase gene families in turnip (*Brassica rapa var. rapa*). *Front. Plant Sci.* **2017**, *8*, 1191. [CrossRef] [PubMed]
36. Yu, Y.H.; Xia, X.L.; Yin, W.L.; Zhang, H.C. Comparative genomic analysis of CIPK gene family in Arabidopsis and Populus. *Plant Growth Regul.* **2007**, *52*, 101–110. [CrossRef]
37. Li, R.F.; Zhang, J.W.; Wei, J.H.; Wang, H.Z.; Wang, Y.Z.; Ma, R.C. Functions and mechanisms of the CBL–CIPK signaling system in plant response to abiotic stress. *Prog. Nat. Sci.* **2009**, *19*, 667–676. [CrossRef]
38. Yu, J.; Wang, J.; Lin, W.; Li, S.G.; Li, H.; Zhou, J.; Ni, P.X.; Dong, W.; Hu, S.N.; Zeng, C.Q.; et al. The Genomes of Oryza sativa: A history of duplications. *PLoS Biol.* **2005**, *3*, e38. [CrossRef]
39. Schlicker, A.; Domingues, F.S.; Rahnenführer, J.; Lengauer, T. A new measure for functional similarity of gene products based on Gene Ontology. *BMC Bioinform.* **2006**, *7*, 302. [CrossRef]
40. Chen, L.; Wang, Q.Q.; Zhou, L.; Ren, F.; Li, D.D.; Li, X.B. Arabidopsis CBL-interacting protein kinase (CIPK6) is involved in plant response to salt/osmotic stress and ABA. *Mol. Biol. Rep.* **2013**, *40*, 4759–4767. [CrossRef]
41. Xu, J.; Li, H.D.; Chen, L.Q.; Wang, Y.; Liu, L.; He, L.; Wu, W. A protein kinase, interacting with two calcineurin b-like proteins, regulates K^+ transporter AKT1 in Arabidopsis. *Cell* **2006**, *125*, 1347–1360. [CrossRef]
42. Chen, L.; Ren, F.; Zhou, L.; Wang, Q.Q.; Zhong, H.; Li, X.B. The *Brassica napus* Calcineurin B-Like 1/CBL-interacting protein kinase 6 (CBL1/CIPK6) component is involved in the plant response to abiotic stress and ABA signalling. *J. Exp. Bot.* **2012**, *63*, 6211–6222. [CrossRef]
43. Batistic, O.; Kudla, J. Plant calcineurin B-like proteins and their interacting protein kinases. *Biochim. Biophys. Acta* **2009**, *1793*, 985–992. [CrossRef]
44. Lan, W.Z.; Lee, S.C.; Che, Y.F.; Jiang, Y.Q.; Sheng, L. Mechanistic analysis of AKT1 regulation by the CBL-CIPK-PP2CA interactions. *Mol. Plant* **2011**, *4*, 527–536. [CrossRef] [PubMed]

45. Weinl, S.; Kudla, J. The CBL–CIPK Ca^{2+}-decoding signaling network: Function and perspectives. *New Phytol.* **2009**, *184*, 517–528. [CrossRef] [PubMed]
46. Finn, R.D.; Clements, J.; Eddy, S.R. HMMER web server: Interactive sequence similarity searching. *Nucleic Acids Res.* **2011**, *39*, W29–W37. [CrossRef] [PubMed]
47. Zhang, T.K.; Liu, C.Y.; Huang, X.B.; Zhang, H.Y.; Yuan, Z.H. Land-plant phylogenomic and pomegranate transcriptomic analyses reveal an evolutionary scenario of *CYP75* genes subsequent to whole genome duplications. *J. Plant Biol.* **2019**, *62*, 48–60. [CrossRef]
48. Edgar, R.C. MUSCLE: Multiple sequence alignment with high accuracy and high throughput. *Nucleic Acids Res.* **2004**, *32*, 1792–1797. [CrossRef]
49. Hartmann, A.; Tesch, D.; Nothwang, H.G.; Binindaemonds, O.R.P. Evolution of the cation chloride cotransporter family: Ancient origins, gene-losses, and subfunctionalization through duplication. *Mol. Biol. Evol.* **2014**, *31*, 434–447. [CrossRef]
50. Minh, B.Q.; Schmidt, H.A.; Chernomor, O.; Schrempf, D.; Woodhams, M.D.; Von Haeseler, A.; Lanfear, R. IQ-TREE 2: New models and efficient methods for phylogenetic inference in the genomic era. *Mol. Biol. Evol.* **2020**, *37*, 1530–1534. [CrossRef]
51. Zhang, C.F.; Zhang, T.K.; Luebert, F.; Xiang, Y.Z.; Huang, C.-H.; Hu, Y.; Rees, M.; Frohlich, M.W.; Qi, J.; Weigend, M.; et al. Asterid phylogenomics/phylotranscriptomics uncover morphological evolutionary histories and support phylogenetic placement for numerous whole genome duplications. *Mol. Biol. Evol.* **2020**, *37*, 3188–3210. [CrossRef]
52. Chen, C.J.; Chen, H.; Zhang, Y.; Thomas, H.R.; Frank, M.H.; He, Y.H.; Xia, R. TBtools: An integrative toolkit developed for interactive analyses of big biological data. *Mol. Plant* **2020**, *13*, 1194–1202. [CrossRef]
53. Wang, Y.P.; Tang, H.B.; Debarry, J.D.; Tan, X.F.; Li, J.; Wang, X.; Lee, T.; Jin, H.; Marler, B.S.; Guo, H. MCScanX: A toolkit for detection and evolutionary analysis of gene synteny and collinearity. *Nucleic Acids Res.* **2012**, *40*, e49. [CrossRef] [PubMed]
54. Feng, Z.T.; Deng, Y.Q.; Fan, H.; Sun, Q.J.; Sui, N.; Wang, B.S. Effects of NaCl stress on the growth and photosynthetic characteristics of *Ulmus pumila* L. seedlings in sand culture. *Photosynthetica* **2014**, *52*, 313–320. [CrossRef]
55. Livak, K.J.; Schmittgen, T.D. Analysis of relative gene expression data using real-time quantitative PCR and the $2^{-\Delta\Delta CT}$ Method. *Methods* **2001**, *25*, 402–408. [CrossRef] [PubMed]
56. Luo, Y.; Qiu, Y.; Na, R.; Meerja, F.; Lu, Q.S.; Yang, C.; Tian, L. A Golden Gate and Gateway double-compatible vector system for high throughput functional analysis of genes. *Plant Sci.* **2018**, *271*, 117–126. [CrossRef] [PubMed]